# Measurement-Protocol Dependence of the Magnetocaloric Effect in Ni-Co-Mn-Sb Heusler Alloys

Salazar Mejia, C.; Kumar, V.; Felser, C.; Skourski, Y.; Wosnitza, J.; Nayak, A. K.;

Originally published:

May 2019

**Physical Review Applied 11(2019), 054006**

DOI: https://doi.org/10.1103/PhysRevApplied.11.054006

# Measurement-protocol dependence of the magnetocaloric effect in Ni-Co-Mn-Sb Heusler alloys

C. Salazar-Mejía,[1,*] V. Kumar,[2] C. Felser,[2] Y. Skourski,[1] J. Wosnitza,[1,3] and A. K. Nayak[4]

[1] *Dresden High Magnetic Field Laboratory (HLD-EMFL), Helmholtz-Zentrum Dresden-Rossendorf, 01328 Dresden, Germany*

[2] *Max Planck Institute for Chemical Physics of Solids, Nöthnitzer Str. 40, 01187 Dresden, Germany.*

[3] *Institut für Festkörper- und Materialphysik, TU Dresden, 01062, Dresden, Germany.*

[4] *School of Physical Sciences, National Institute of Science Education and Research (NISER), Bhubaneswar, Jatni 752050, India.*

(Dated: April 29, 2019)

Ni-Co-Mn-Sb-based Heusler shape-memory alloys that undergo a martensitic-structural transition around room temperature are well known for exhibiting large magnetic entropy change and elastocaloric effect. Here, we report the observation of a large adiabatic temperature change of -11 K in Ni-Co-Mn-Sb system by using direct adiabatic temperature-change measurements in pulsed-magnetic fields. We show that a large magnetic cooling can be achieved in a wide temperature range spanning from 120 to 270 K by purposefully varying the chemical composition. The temperature- and field-dependent irreversibility of the effect is analyzed through a detailed experimental study of the protocol-dependent magnetocaloric effect. The present study is an important contribution towards the understanding of irreversible magnetocaloric effects in materials with magneto-structural transition.

## I. INTRODUCTION

It has been proposed that solid-state based magnetic cooling has enough potential to replace the conventional gas-based cooling technique [1–3]. However, most of the magnetic materials showing a large magnetocaloric effect (MCE) contain rare-earth elements [2, 4]. In recent years, it has been found that some of the transition-metal-based Heusler shape-memory materials exhibit a large MCE comparable to that of the rare-earth-based systems [5–7]. However, thermal hysteresis is a critical issue for the performance of cooling devices based on the magnetocaloric effect [8–11]. Specifically, in the case of Heusler alloys that undergo a first-order magnetostructural transition, thermal hysteresis, intrinsic of the transition, not only lead to irreversible effects, but to magnetocaloric properties that strongly depend on the measurement protocol at which they are obtained, for instance, whereas the initial temperature is approached on cooling or on heating [12–14]. As a consequence, the temperature-dependent adiabatic temperature change ($\Delta T_{ad}$) and isothermal entropy change ($\Delta S_{iso}$) of Heusler alloys exhibit, likewise, thermal hysteresis and are protocol dependent [11, 13, 15–19]. This is commonly overlooked in the literature, especially when calculating the magnetocaloric properties from indirect measurements. However, hysteresis should be always taken in consideration in order to properly characterize a magnetocaloric material, such as reported for FeRh [20], LaFeSi [14, 21, 22], NiMnGa [21], and Ni(Co)MnIn [12, 17], among others. The recently proposed approach that considers the hysteresis on Heusler alloys as a desirable property to be exploited in multicaloric cooling cycles [23], also supports the necessity to properly characterize the magnetocaloric effect in first-order materials.

Among the Heusler shape-memory materials, Ni-Co-Mn-Sb-based alloys have been widely studied. It has been shown that members of this family exhibit, among other phenomena, elastocaloric [24], magnetocaloric [25, 26], and shape-memory [26, 27] effects at room temperature. Ni-Co-Mn-Sb alloys have further been shown to display exchange bias [28] and kinetic arrest [29]. In general, the $Ni_{50-x}Co_xMn_{38}Sb_{12}$ alloys (with $x$ = 5, 6, and 7) undergo at $T_M$ a first-order martensitic transition from a high-temperature ferromagnetic austenite to a low-temperature martensitic phase, which exhibits lower magnetic moment. Thus, the ferromagnetic transition at $T_C$ appears above $T_M$. The increase of Co content shifts the martensitic transition toward lower temperatures while increasing slightly the ferromagnetic transition temperature [27, 30]. The broadness of the transition also increases with Co content. Although a large MCE, specifically, a large magnetic entropy change determined from indirect measurements, have been reported for the Ni-Co-Mn-Sb system, direct measurements of the adiabatic temperature change have not been reported. In this work, we report the adiabatic temperature change, $\Delta T_{ad}(T)$, of the Heusler alloys $Ni_{50-x}Co_xMn_{38}Sb_{12}$ with $x = 5$, 6, and 7, through direct measurements in pulsed-magnetic fields up to 20 T. In order to properly characterize MCE materials, high fields (above 2 T) are often needed to completely induce the transition and, in that way, avoid entering in a minor cycle or in a mixed state. Additionally, measurements under high magnetic fields will give information such as on the maximum $\Delta T_{ad}$ value at the transition, as the maximum temperature range where these values can be achieved, the field dependence of the transition temperatures, and the temperature region where the effect is reversible. The latter point, i.e., the irreversibility of the effect, is analyzed. Furthermore,

* c.salazar-mejia@hzdr.de

a detailed experimental study of the protocol-dependent MCE of $Ni_{45}Co_5Mn_{38}Sb_{12}$ is presented. $\Delta T_{ad}$ for this alloy was characterized following different measurement protocols and a large difference between $\Delta T_{ad}$ recorded using cooling protocol and those recorded using heating protocol is reported.

## II. EXPERIMENTAL

Polycrystalline ingots of $Ni_{50-x}Co_xMn_{38}Sb_{12}$, $x = 5$, 6, and 7, were prepared following Ref. 30. Magnetization measurements were carried out in a physical property measurement system (Quantum Design). Direct measurements of $\Delta T_{ad}$ were performed in a home-built experimental setup in pulsed magnetic fields at the Dresden High Magnetic Field Laboratory (HLD). Short pulse durations (20-50 ms) not only allow for adiabatic conditions, making possible to measure $\Delta T_{ad}$ without heat losses, but also probes the thermal kinetics of materials on a time scale matching the one suitable for applications, i.e. 1-100 Hz [31]. Additionally, the high fields available allow, in this case, to induce the martensitic transition over a wide temperature range.

## III. RESULTS AND DISCUSSION

Temperature-dependent magnetization curves $M(T)$ for the three different Co concentrations are presented in Fig. 1. $M(T)$ data were recorded on cooling and subsequent heating for applied magnetic fields of 0.01, 2, 6, and 14 T. $Ni_{45}Co_5Mn_{38}Sb_{12}$ [Fig. 1(a)], undergoes a martensitic transition at $T_M = 252.5$ K from a high-temperature ferromagnetic austenite to a low-temperature ferrimagnetic martensitic phase, which exhibits a lower magnetic moment. A thermal hysteresis of around 11 K is intrinsic to the first-order magnetostructural transition and the reverse transition takes place upon heating around $T_A = 264$ K. The Curie temperature is $T_C = 344$ K. With increasing Co content, $T_C$ slightly increases, for instance, for $x = 6$ $T_C \approx 350$ K. Concomitantly, the martensitic transition is shifted toward lower temperatures, as previously reported [27, 30]. Specifically, for $x = 6$ and $x = 7$, the martensitic transition takes place upon cooling at around 212 K [Fig. 1(b)] and 179 K [Fig. 1(c)], respectively. At the same time, the transition broadens as Co increases, while the hysteresis of the transition remains almost constant.

Magnetic field stabilizes the higher-moment magnetic phase, in this case the austenite. Therefore, the martensitic transition shifts toward lower temperature with field, as shown for all samples in Fig. 1 and specifically in the inset, where the field dependence of $T_M$ is plotted. The sensitivity of the transition to the magnetic field is quantified by $dT_M/dH$, which is -1.7, -2.2, and -3.2 K/T for $x = 5$, 6, and 7, respectively. This is a rather weak field dependence compared with other Heusler alloys [19, 32].

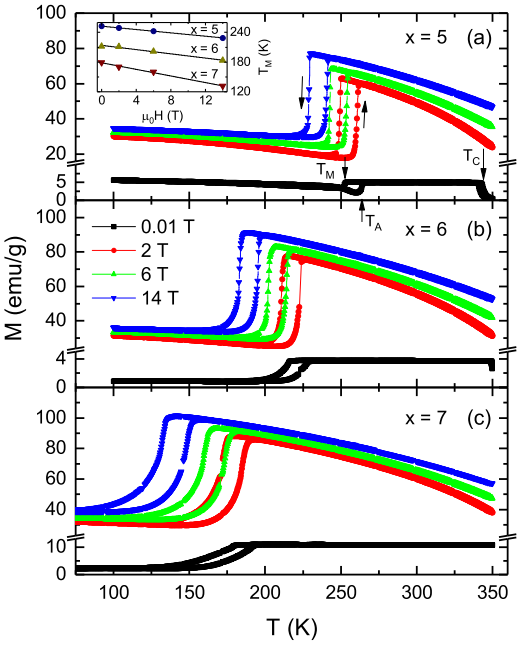


FIG. 1. Temperature-dependent magnetization curves of (a) $Ni_{45}Co_5Mn_{38}Sb_{12}$, (b) $Ni_{44}Co_6Mn_{38}Sb_{12}$, and (c) $Ni_{43}Co_7Mn_{38}Sb_{12}$, recorded at 0.01, 2, 6, and 14 T during cooling and heating. The inset shows the field dependence of $T_M$ for the three samples.

It is worth to mention, that the martensite to austenite transition in these materials can be induced by large magnetic fields even at low temperatures [33].

The adiabatic temperature change $\Delta T_{ad}(T)$ was measured for all samples close to the martensitic transition. The results are presented in Fig. 2. Magnetic-field pulses of 6 and 20 T were applied. Thereby, the sample was always heated up to the austenitic phase and cooled down to the martensitic phase before reaching the temperature $T_i$. This was done in order to erase the sample history. Additionally, for $x = 6$ and 7, some 6 T pulses were performed without heating or cooling the sample between pulses, in order to study the history dependence (repeated pulses in Fig. 2).

$\Delta T_{ad}$ was determined for field up and down sweeps to study the irreversibility of the effect. This is exemplified in the inset of Fig. 2, where raw data $\Delta T_{ad}$ as a function of time for $x = 6$ at $T_i = 220$ K and a field change of 20 T are presented. The time-dependent magnetic field is also plotted (hatched area). As expected, for temperatures below and around the martensitic transition, the samples exhibit an inverse MCE, i.e., $\Delta T_{ad}$ decreases for up sweeps ($0 \rightarrow 6/20$ T). During the down sweeps ($6/20$ T $\rightarrow 0$), the samples heat up. Depending on $T_i$ and the field strength, the samples can return back to $T_i$, showing then a reversible effect, or to a final temperature $T_f \neq T_i$, exhibiting an irreversible effect. For temperatures that lie in the hysteresis region, the effect is irreversible for the first application of field, specially

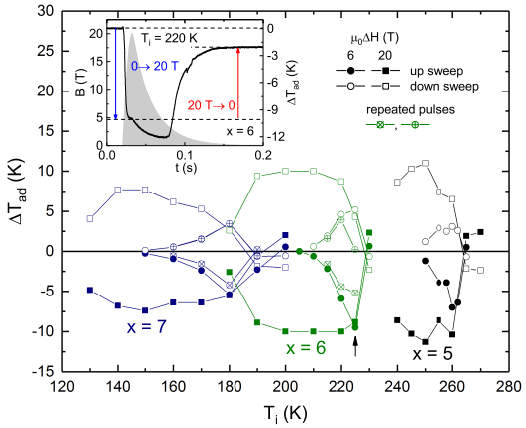


FIG. 2. Adiabatic temperature change of $Ni_{45}Co_5Mn_{38}Sb_{12}$ (black), $Ni_{44}Co_6Mn_{38}Sb_{12}$ (green) and $Ni_{43}Co_7Mn_{38}Sb_{12}$ (blue) near the martensitic transformations, obtained for magnetic field pulses of 6 (circles) and 20 T (squares). Closed symbols indicate $\Delta T_{ad}$ values obtained for field up and open symbols for down sweeps. The inset shows the recorded time-dependent data of $\Delta T_{ad}$ at the initial temperature $T_i = 220$ K for $x = 6$, together with the time-dependent magnetic field.

apparent for 6 T pulses.

For a field change of 20 T, the alloy with $x = 5$ exhibits the largest $\Delta T_{ad} = -11.3$ K (up sweep). However, for a field change of 6 T, the alloy with $x = 6$ shows the largest effect of $\Delta T_{ad} = -9.5$ K at $T_i = 225$ K (marked by an arrow in Fig. 2). At this specific temperature, the MCE is irreversible: after down sweep, the sample heats up by only $\Delta T_{ad} = 5.2$ K. When the field pulse is repeated without heating the sample above $T_C$, the sample cools down by only $-5.2$ K. In the subsequent down sweep no MCE is recorded. This shows that the MCE effect is highly irreversible in these alloys and depends strongly on the measurement history, as previously reported [6, 27]. This irreversibility in the MCE in combination with large shape-memory effects [27], makes these materials potential candidates to be used in a multicaloric cooling cycle (based on magneto- and elasto-caloric effects), where thermal hysteresis is exploited [23].

We have previously reported on a large relative length change of up to 1 % on the alloys with $x = 5$ and $x = 6$ due to the magnetic-field-induced martensitic transition. Specifically, for the $x = 5$ alloy, a one-way magnetic shape-memory effect was found at $T_i = 258$, 260, and 262 K. The initial application of the magnetic field induces the martensite transition that leads to an expansion of the sample. Upon subsequent field sweeps, the length of the sample stays almost constant indicating that the material remains in the austenitic phase [27]. As shown in Fig. 2, at these temperatures, the $x = 5$ alloy also shows large irreversibility. For example, at $T_i = 260$ K, the sample cools down by 7 K in the up-sweep, but warms up by only 3.1 K in the down-sweep, indicating that almost half of the sample stays in the austenitic phase. Simultaneous measurements of the magnetostriction and the adiabatic temperature change could shed more light into the correlation between length and temperature change in these alloys.

$Ni_{45}Co_5Mn_{38}Sb_{12}$ shows a large difference in the MCE for field pulses of 6 and 20 T, as 6 T is not sufficient to induce the transition in the investigated temperature range, while 20 T is, as will be discussed later. The alloys with $x = 6$ and 7 show a higher sensitivity of the transition to the field $dT_M/dH$ (see inset of Fig. 1) so that close to $T_M$ 6 T is sufficient to induced the transition.

The samples exhibit broad $\Delta T_{ad}(T)$ plateaus for the 20 T pulses that extend approximately in the temperature range from 245 to 260 K for $x = 5$, 190 to 225 K for $x = 6$, and 130 to 180 K for $x = 7$. The latter alloy has a broader transition leading to a MCE that extends over a large temperature range. Furthermore, the $\Delta T_{ad}$ values found in these alloys are among the largest found so far under high magnetic fields [6, 34–37].

In general, the magnetocaloric effect decreases as $x$ increases, as shown in Fig. 2. This is related to the fact that $|T_C - T_M|$ increases with Co substitution (Fig. 1) and, due to the contradictory role of the magnetic and structural contributions to the magnetocaloric effect in metamagnetic $Ni_2Mn$-based Heusler alloys, the MCE also decreases [38, 39].

We have chosen the $x = 5$ sample to study the measurement-protocol dependence of the MCE. Prior to the $\Delta T_{ad}$ characterization, isothermal magnetization curves $M(H)$ were measured. These measurements allow to estimate the MCE expected at different temperatures, although dynamic effects due to the field-sweep rates and differences between isothermal and adiabatic measurements cannot be ruled out. Figure 3 shows $M(H)$ at 250 K, 254 K, and 259 K, recorded up to 14 T in static fields for different measurement protocols: (i) $T_i$ reached on discontinuous cooling, (ii) $T_i$ reached on discontinuous heating, and (iii) $T_i$ reached on continuous heating. In the first two protocols, the sample is always heated up to the austenitic phase and cooled down to the martensitic phase (or *vice versa*) before reaching the initial temperature $T_i$. In the case of continuous heating, $T_i$ is just approached heating directly from the previously measured temperature. The transition region of the 0.01 T $M(T)$ curve is shown in the inset Fig. 3(d), where additionally, the austenitic start/finish temperature $T_A^S = 260$ K/$T_A^F = 265$ K and the martensitic start/finish temperature $T_M^S = 253$ K/$T_M^F = 251$ K are indicated. These temperatures characterized the martensitic transition. At 250 K ($T < T_A^S$, $T < T_M^F$), both curves, measured on cooling and on heating, are almost the same [Fig. 3(a)], as the sample is mainly in the martensitic state for both cases before applying field. The small difference between the curves arises from the fact that the thermal hysteresis loop is not completely closed at this temperature and some little amount of austenite state could be still present when $T_i$ is reached on cooling. The transition from martensite to austenite

is induced by around 6.5 T. Under field removal, the sample transformed back to the martensitic phase at around 2.5 T. Indeed, a field of 9 T is sufficient to complete the field-induced martensitic transition.

For the second case [see Fig. 3(b)], 254 K was reached on (i) cooling from 350 K, (ii) on heating from 100 K, and (iii) on heating directly after measuring $M(H)$ at 250 K (continuous heating). 254 K lies below the austenitic start temperature $T < T_A^S$ and just between $T_M^F$ and $T_M^S$, the martensitic finish and start temperatures, respectively. Therefore, there is a small difference between the measurements performed on cooling and heating. In the case (i), the sample is in a mixture of austenitic and martensitic phases before the measurement, while in the case (ii) the sample starts from a pure martensitic phase. In the case (iii), discontinuous heating, the results differ slightly from case (ii) as some austenitic phase (with higher magnetic moment) is retained in the sample from the previous measurement at 250 K.

Figure 3(c) shows the results for the $M(H)$ curves recorded at 259 K under the same conditions explained above. This temperature is just below $T_A^S$ and the difference between the measurements performed using the discontinuous heating and continuous heating protocols is notable. In the case of continuous heating, some austenitic phase is already present in the sample before applying field as a result of the previous $M(H)$ measurement at 254 K. Therefore, the induced transition takes place at lower critical field. When the temperature is reached on cooling, the sample is in the austenitic ferromagnetic state, as 259 K lies above $T_M^S = 253$ K, so no induced transition is observed when applying the field, as shown in the inset Fig. 3(e).

In a next step, we have characterized $\Delta T_{ad}(T)$ of $Ni_{45}Co_5Mn_{38}Sb_{12}$ following discontinuous heating and discontinuous cooling protocols as well as a continuous heating protocol. $\Delta T_{ad}(T)$ was determined under applied fields of 2, 6, and 20 T and the results are presented in Fig. 4.

First thing to notice is that there is a big difference on the $\Delta T_{ad}(T)$ obtained using heating protocol and those measured using cooling protocol. The curves are shifted in temperature, as expected. This temperature difference between the curves follows the thermal hysteresis observed in the $M(T)$ curves. In a general picture, the martensitic transition can be induced by magnetic field. Specifically, the sample transforms from the martensitic to the austenitic phase, as field stabilizes the higher-moment phase. Consequently, on cooling, the induced transition could only take place below $T_M^S$ (where some martensitic phase starts being present in the sample) and, on heating, the transition can be induced up to a temperature $T_A^F$ (inset Fig. 4). As $T_M^S < T_A^F$, both $\Delta T_{ad}(T)$ curves, recorded using cooling and using heating protocols, extent over different temperature ranges. For results obtained at 2 T, the curves are separated about 10 K, while it decreases to about 8 and 6 K for field changes of 6 and 20 T, respectively. Additionally, there is a large

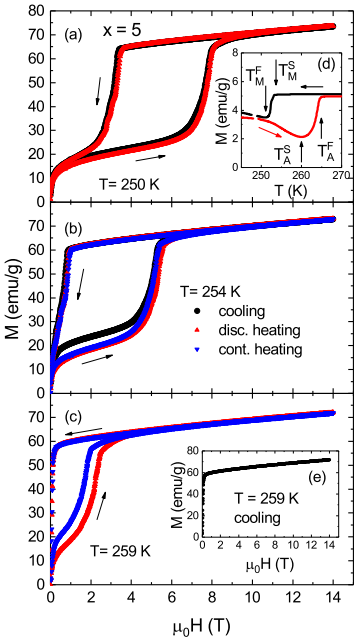


FIG. 3. Isothermal magnetization curves of $Ni_{45}Co_5Mn_{38}Sb_{12}$ recorded at (a) 250 K, (b) 254 K, and (c) and (e) 259 K following different protocols. Inset (d) shows $M(T)$ around the martensitic transition at 0.01 T where the characteristic temperatures are marked. See text for details.

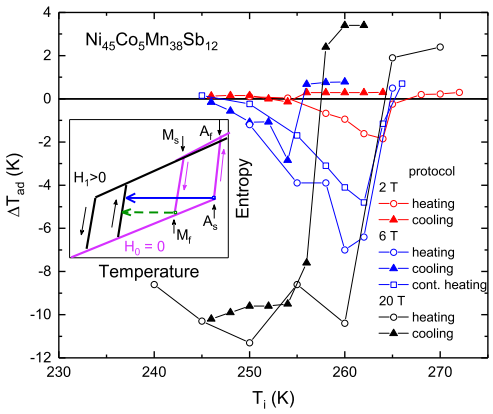


FIG. 4. Adiabatic temperature change of $Ni_{45}Co_5Mn_{38}Sb_{12}$ around the martensitic transformation, obtained under magnetic field pulses of 2, 6, and 20 T following discontinuous heating (circles) and discontinuous cooling (triangles). For a field change of 6 T also continuous heating data were recorded (squares). Inset: schematic of the adiabatic cooling in case of using heating- (continuous blue arrow) or cooling- (discontinuous green arroy) protocol. See text for details.

difference in the maximum $\Delta T_{ad}$ values obtained upon heating and those achieved upon cooling. This can be understand with the help of the schematic of the entropy curves for the case of the martensitic first-order transition at $H_0 = 0$ and $H_1 > 0$ show in the inset of Fig. 4. In

this schematic, the hysteresis of the transition has been taken in consideration [12]. The $\Delta T_{ad}$ values obtained using cooling protocol (illustrated with the discontinuous green line) are limited, among other parameters, for the width of the hysteresis. In general, a larger MCE is found using heating protocol (illustrated as the continuous blue line) in comparison to the MCE measured using cooling.

From $M(H)$ presented in Fig. 3, one can see that 2 T is not sufficient to complete the martensitic transition. Consequently, the MCE on heating is small. When measuring using the cooling protocol, the MCE is negligible.

A field change of 6 T only induce the transition in a narrow temperature range (Fig. 3). The maximum $\Delta T_{ad}$ differs strongly for the heating and cooling protocols. For instance, for the cooling protocol, the maximum $\Delta T_{ad}$ is $-2.8$ K reached at 254 K, while for the heating protocol, $\Delta T_{ad}$ is up to 2.5 times larger with -7 K at 260 K.

Furthermore, measurements for $\mu_0 \Delta H = 6$ T following the continuous heating protocol were performed. As found earlier, the results obtained in this way depend on the temperature steps at which the measurements are taken, i.e., each $\Delta T_{ad}$ depends on the previous one [12], therefore, results obtained this way have to be considered carefully. The $\Delta T_{ad}$ values obtained using this method are lower than the ones obtained under discontinuous heating as the previous field application induces partially, or completely, the transition to the austenitic phase and some of the austenite is retained after field removal [27, 29]. This arrested austenite (not presence in the case of discontinuous heating) does not contribute to the cooling MCE.

For field pulses of 20 T, the adiabatic temperature change has a maximum $\Delta T_{ad} = -11.3$ K, as the field is large enough to induce the transition in the measurement temperature range (see Fig. 3). It is important to notice that for the 20 T pulses the MCE is almost reversible (see for instance the data for up and down sweeps in Fig. 2). Even a field change of 10 T is sufficient to induce and complete the transition, as seen in Fig. 3. Thus, this large $\Delta T_{ad}$ would also be achieved with smaller fields of 10 T.

## IV. CONCLUSIONS

To summarize, we have investigated the magnetocaloric effect of the Heusler alloys $Ni_{45}Co_5Mn_{38}Sb_{12}$, $Ni_{44}Co_6Mn_{38}Sb_{12}$, and $Ni_{43}Co_7Mn_{38}Sb_{12}$ for magnetic field changes of 2, 6, and 20 T. For a field change of 20 T, $Ni_{45}Co_5Mn_{38}Sb_{12}$ exhibits the largest MCE of -11.3 K, however, $Ni_{44}Co_6Mn_{38}Sb_{12}$ exhibits the largest MCE for 6 T, -9.5 K. A detailed study on the measurement-protocol dependence of the MCE of $Ni_{45}Co_5Mn_{38}Sb_{12}$ was performed. A large difference between $\Delta T_{ad}$ recorded using cooling protocol and those recorded using heating protocol is found. The reversibility and reproducibility of the magnetocaloric effect strongly depends on the thermal hysteresis and the sensitivity to the field of the martensitic transition. The magnetocaloric effect also depends on the measuring protocol. Our results show that the thermal hysteresis of the first-order transition should always be considered when investigating the MCE in Heusler alloys.

## ACKNOWLEDGMENTS

We acknowledge the support of the HLD at HZDR, member of the European Magnetic Field Laboratory (EMFL).

[1] B. Yu, M. Liu, P. W. Egolf, and A. Kitanovski, "A review of magnetic refrigeration and heat pump prototypes built before the year 2010," Int. J. Refrig. **33**, 1029–1060 (2010).

[2] O. Gutfleisch, M. A. Willard, E. Brück, C. H. Chen, S. G. Sankar, and J. P. Liu, "Magnetic materials and devices for the 21st century: Stronger, lighter, and more energy efficient," Adv. Mater. **23**, 821–842 (2011).

[3] E. Brück, "Developments in magnetocaloric refrigeration," J. Phys. D: Appl. Phys. **38**, R381 (2005).

[4] V. Franco, J. S. Blazquez, J. J. Ipus, J. Y. Law, L. M. Moreno-Ramirez, and A. Conde, "Magnetocaloric effect: from materials research to refrigeration," Prog. Mater. Sci. **93**, 112–232 (2018).

[5] T. Krenke, E. Duman, M. Acet, E. F. Wassermann, X. Moya, L. Mañosa, and A. Planes, "Inverse magnetocaloric effect in ferromagnetic Ni-Mn-Sn alloys," Nat. Mater. **4**, 450–454 (2005).

[6] M. Ghorbani Zavareh, C. Salazar Mejía, A. K. Nayak, Y. Skourski, J. Wosnitza, C. Felser, and M. Nicklas, "Direct measurement of the magnetocaloric effect in the Heusler alloy $Ni_{50}Mn_{35}In_{15}$ in pulsed magnetic fields," Appl. Phys. Lett. **106**, 071904 (2015).

[7] J. Liu, T. Gottschall, K. P. Skokov, J. D. Moore, and O. Gutfleisch, "Giant magnetocaloric effect driven by structural transitions," Nat. Mater. **11**, 620–626 (2012).

[8] O. Gutfleisch, T. Gottschall, M. Fries, D. Benke, I. Radulov, K. P. Skokov, H. Wende, M. Gruner, M. Acet, P. Entel, and M. Farle, "Mastering hysteresis in magnetocaloric materials," Phil. Trans. R. Soc. A **374**, 20150308 (2016).

[9] L. von Moos, C. R. H. Bahl, K. K. Nielsen, and K. Engelbrecht, "The influence of hysteresis on the determination of the magnetocaloric effect in $Gd_5Si_2Ge_2$," J. Phys. D: Appl. Phys. **48**, 025005 (2015).

[10] F. Guillou, H. Yibole, G. Porcari, L. Zhang, N. H. van Dijk, and E. Brück, "Magnetocaloric effect, cyclability and coefficient of refrigerant performance in the MnFe(P, Si, B) system," J. Appl. Phys. **116**, 063903 (2014).

[11] I. Titov, M. Acet, M. Farle, D. Gonzalez-Alonso, L. Mañosa, A. Planes, and T. Krenke, "Hysteresis effects in the inverse magnetocaloric effect in martensitic Ni-Mn-In and Ni-Mn-Sn," J. Appl. Phys. **112**, 073914 (2012).

[12] T. Gottschall, K. P. Skokov, R. Burriel, and O. Gutfleisch, "On the S(T) diagram of magnetocaloric materials with first-order transition: Kinetic and cyclic effects of Heusler alloys," Acta Mater. **107**, 1–8 (2016).

[13] A. Ghosh, P. Sen, and K. Mandal, "Measurement protocol dependent magnetocaloric properties in a Si-doped Mn-rich MnNi-Sn-Si off-stoichiometric Heusler alloy," J. Appl. Phys. **119**, 183902 (2016).

[14] B. Kaeswurm, V. Franco, K. P. Skokov, and O. Gutfleisch, "Assessment of the magnetocaloric effect in La,Pr(Fe,Si) under cycling," J. Magn. Magn. Mater. **406**, 259–265 (2016).

[15] V. Basso, C. P. Passo, K. P. Skokov, O. Gutfleisch, and V. V. Khovaylo, "Hysteresis and magnetocaloric effect at the magnetostructural phase transition of Ni-Mn-Ga and Ni-Mn-Co-Sn heusler alloys," Phys. Rev. B **85**, 014430 (2012).

[16] V. V. Khovaylo, K. P. Skokov, O. Gutfleisch, H. Miki, R. Kainuma, and T. Kanomata, "Reversibility and irreversibility of magnetocaloric effect in a metamagnetic shape memory alloy under cyclic action of a magnetic field," Appl. Phys. Lett. **97**, 052503 (2010).

[17] J. Liu, N. Scheerbaum, J. Lyubina, and O. Gutfleisch, "Reversibility of magnetostructural transition and associated magnetocaloric effect in NiMnInCo," Appl. Phys. Lett. **93**, 102512 (2008).

[18] F. Scheibel, T. Gottschall, A. Taubel, M. Fries, K. P. Skokov, A. Terwey, W. Keune, K. Ollefs, H. Wende, M. Farle, M. Acet, O. Gutfleisch, and M. E. Gruner, "Hysteresis design of magnetocaloric materials-from basic mechanisms to applications," Energy Technol. **6**, 1397–1428 (2018).

[19] A. Taubel, T. Gottschall, M. Fries, S. Riegg, C. Soon, K. P. Skokov, and O. Gutfleisch, "A comparative study on the magnetocaloric properties of Ni-Mn-X(-Co) Heusler alloys," Phys. Status Solidi B **255**, 1700331 (2018).

[20] A. Chirkova, K. P. Skokov, L. Schultz, N. V. Baranov, O. Gutfleisch, and T. G. Woodcock, "Giant adiabatic temperature change in FeRh alloys evidenced by direct measurements under cyclic conditions," Acta Mater. **106**, 15–21 (2016).

[21] K. P. Skokov, V. V. Khovaylo, K. H. Müller, J. D. Moore, J. Liu, and O. Gutfleisch, "Magnetocaloric materials with first-order phase transition: thermal and magnetic hysteresis in $LaFe_{11.8}Si_{1.2}$ and $Ni_{2.21}Mn_{0.77}Ga_{1.02}$ (invited)," J. Appl. Phys. **111**, 07A910 (2012).

[22] K. P. Skokov, K.-H. Müller, J. D. Moore, J. Liu, A. Yu. Karpenkov, M. Krautz, and O. Gutfleisch, "Influence of thermal hysteresis and field cycling on the magnetocaloric effect in $LaFe_{11.6}Si_{1.4}$," J. Alloys Comp. **552**, 310–317 (2013).

[23] T. Gottschall, A. Gracia-Condal, M. Fries, A. Taubel, L. Pfeuffer, Ll. Mañosa, A. Planes, K. P. Skokov, and O. Gutfleisch, "A multicaloric cooling cycle that exploits thermal hysteresis," Nat. Mater. **17**, 929 (2018).

[24] R. Millán-Solsona, E. Stern-Taulats, E. Vives, A. Planes, J. Sharma, A. K. Nayak, K. G. Suresh, and L. Mañosa, "Large entropy change associated with the elastocaloric effect in polycrystalline Ni-Mn-Sb-Co magnetic shape memory alloys," Appl. Phys. Lett. **105**, 241901 (2014).

[25] A. K. Nayak, K. G. Suresh, and A. K. Nigam, "Giant inverse magnetocaloric effect near room temperature in Co substituted NiMnSb Heusler alloys," J. Phys. D: Appl. Phys. **42**, 035009 (2009).

[26] J. Du, Q. Zheng, W. J. Ren, W. J. Feng, X. G. Liu, and Z. D. Zhang, "Magnetocaloric effect and magnetic-field-induced shape recovery effect at room temperature in ferromagnetic Heusler alloy Ni-Mn-Sb," J. Phys. D: Appl. Phys. **40**, 18 (2007).

[27] C. Salazar Mejia, R. Küchler, A. K. Nayak, C. Felser, and M. Nicklas, "Uniaxial-stress tuned large magnetic-shape-memory effect in Ni-Co-Mn-Sb Heusler alloys," Appl. Phys. Lett. **110**, 071901 (2017).

[28] A. K. Nayak, K. G. Suresh, and A. K. Nigam, "Observation of enhanced exchange bias behaviour in NiCoMnSb heusler alloys," J. Phys. D: Appl. Phys. **42**, 115004 (2009).

[29] A. K. Nayak, K. G. Suresh, and A. K. Nigam, "Phase coexistence induced by cooling across the first order transition in NiCoMnSb shape memory alloy," J. Appl. Phys. **108**, 063915 (2010).

[30] A. K. Nayak, K. G. Suresh, and A. K. Nigam, "Magnetic, electrical, and magnetothermal properties in Ni-Co-Mn-Sb Heusler alloys," J. Appl. Phys. **107**, 09A927 (2010).

[31] M. D. Kuzmin, "Factors limiting the operation frequency of magnetic refrigerators," Appl. Phys. Lett. **90**, 251916 (2007).

[32] M. Acet, Ll. Mañosa, and A. Planes, "Magnetic-field-induced effects in martensitic Heusler-based magnetic shape memory alloys," Magnetic-field-induced Effects In Martensitic Heusler-based Magnetic Shape Memory Alloys, Handbook Mag. Mater. **19**, 231–289 (2011).

[33] A. K. Nayak, C. Salazar Mejia, S. W. D′Souza, S. Chadov, Y. Skourski, C. Felser, and M. Nicklas, "Large field-induced irreversibility in Ni-Mn based Heusler shape-memory alloys: A pulsed magnetic field study," Phys. Rev. B **90**, 220408 (2014).

[34] M. Ghorbani Zavareh, Y. Skourski, K. P. Skokov, D. Yu. Karpenkov, L. Zvyagina, A. Waske, D. Haskel, M. Zhernenkov, J. Wosnitza, and O. Gutfleisch, "Direct measurement of the magnetocaloric effect in $La(Fe,Si,Co)_{13}$ compounds in pulsed magnetic fields," Phys. Rev. Appl. **8**, 014037 (2017).

[35] Y. Koshkid′ko, S. Pandey, A. Quetz, A. Aryal, I. Dubenko, J. Cwik, E. Dilmieva, A. Granovsky, E. Lahderanta, A. Zhukov, S. Stadler, and N. Ali, "Inverse magnetocaloric effects in metamagnetic Ni-Mn-In-based alloys in high magnetic fields," J. Alloy Compd. **695**, 3348–3352 (2017).

[36] T. Kihara, X. Xu, W. Ito, R. Kainuma, and M. Tokunaga, "Direct measurements of inverse magnetocaloric effects in metamagnetic shape-memory alloy NiCoMnIn," Phys. Rev. B **90**, 214409 (2014).

[37] A. P. Kamantsev, V. V. Koledov, A. V. Mashirov, E. T. Dilmieva, V. G. Shavrov, J. Cwik, A. S. Los, V. I. Nizhankovskii, K. Rogacki, I. S. Tereshina, Y. S. Koshkid′ko, M. V. Lyange, V. V. Khovaylo, and P. Ari-Gur, "Magnetocaloric and thermomagnetic properties of $Ni_{2.18}Mn_{0.82}Ga$ heusler alloy in high magnetic fields up to 140 kOe," J. Appl. Phys. **117**, 163903 (2015).

[38] C. Salazar Mejía, M. Ghorbani Zavareh, A. K. Nayak, Y. Skourski, J. Wosnitza, C. Felser, and M. Nicklas,

"Pulsed high-magnetic-field experiments: New insights into the magnetocaloric effect in Ni-Mn-In Heusler alloys." J. Appl. Phys. **117**, 17E710 (2015).

[39] T. Gottschall, K. P. Skokov, D. Benke, M. E. Gruner, and O. Gutfleisch, "Contradictory role of the magnetic contribution in inverse magnetocaloric Heusler materials," Phys. Rev. B **93**, 184431 (2016).